MULTI-OBJECTIVE OPTIMIZATION FOR PRELIMINARY DESIGN OF ROCKET TURBINE ENGINE USING AN EVOLUTIONARY ALGORITHM

Marco A. H. Cunha, awallon@ita.br
Liquid Propulsion Laboratory - LPL / IAE-DCTA

Jesuino Takachi Tomita, jtakachi@ita.br
Technological Institute of Aeronautics - ITA/DCTA

Abstract.*This work purposes a study on a preliminary design in rocket turbine engine comparing the highest efficient against a lightweight aerodynamic configuration for aerospace endeavors. A framework has been developed based on a fast elitist non-dominated sorted genetic algorithm, well-known as NSGA-II. The Pareto-optimal set yielded is evaluated by a straightforward search method that sorts by mass increase a vector of solutions for a turbopump power-balance requirement of* 1.2 *MW. The mass takes into account the overall dimensions of a rotor wheel involving thus, sensitive-weight design parameters aerodynamically optimized. The objective functions are based on empirical and semi-empirical correlations. Results of performance have revealed great agreements with existing works in the field. It was observed that the highest efficiency solution identified does not have lightweight characteristics since it is accomplished by a penalties especially when analyzed from a strength standpoint whereas a possible lightweight solution is limited by both efficiency and strength standpoints. Finally, the multi-objective approach utilized herein brings out new insights into the space solution allowing to point out a solution as close as possible to a desired trade decision.*

Keywords: *multi-objective optimization, liquid-propellant turbines, genetic algorithms, convex optimization*

NOMENCLATURE

MOO	=	multi-objective optimization	*EA*	=	evolutionary algorithm
MOEA	=	multi-objective evolutionary algorithm	*POF*	=	pareto-optimal front
LPRE	=	liquid propellant rocket engine	u	=	peripheral velocity, m/s
u/c_{ad}	=	isentropic velocity ratio	$\overline{L}_u$	=	coefficient of circular work
η_u	=	circular efficiency	L^*_{ad}	=	adiabatic work, J/kg
θ	=	flow turning angle, $degrees$	p^*_0	=	gas generator pressure, Pa
$p2$	=	outlet pressure, Pa	$p2/p^*_0$	=	pressure drop
$\dot{m}$	=	mass flow rate, kg/s	ω	=	angular velocity, rad/s^{-1}
N_T	=	effective power, $watts$	η_T	=	effective efficiency
z_r	=	rotor blade account	ρ_t	=	expansion degree
t/b	=	pitch-to-chord ratio	ξ_p	=	profile losses
α_1	=	stator outlet angle	δ_r	=	radial clearence, m
Δ_z	=	axial clearence, m	ΔH_p	=	periphery overlap, m
ΔH_{bt}	=	periphery overlap, m	$\overline{h}$	=	relative height
$\overline{b}_{sh}$	=	reduced shroud width	ρ_T	=	reaction degree (or expansion degree)
ι	=	incidence angle	b_p	=	adjusted blade chord, m
c_{max}	=	maximum thickness of blade, m	h_p	=	average height, m
ι	=	incidence angle	b_p	=	adjusted blade chord, m
$_d$	=	died wheel diameter, m	δ	=	wheel thickness, m
$\rho_{.m}$	=	material density, kg/m^3	a	=	throat area, m^2
t	=	blade-to-blade pitch, m	χ	=	setting angle
D_{cp}	=	mean diameter, m	ϵ	=	admission degree
n_{st}	=	power-speedy coefficient	h_{1p}	=	span of blade, m
φ	=	stator velocity factor	C_{fdsk}	=	disk friction coefficient
C_{fsh}	=	shroud friction coefficient	G	=	mass flow rate, kg/s
σ_1	=	stator pressure drop	$q_{(\lambda c1)}$	=	reduced absolut velocity, m/s
σ_2	=	rotor pressure drop	Gy	=	leakage flow rate over shroud, kg/s
μ_{3a3}	=	labyrinth coefficient	η_p	=	flow rate efficiency of rotor
ψ	=	supersonic velocity factor	c_1	=	outlet stator absolute velocity, m/s
β_1	=	inlet relative flow angle	β_2	=	outlet relative flow angle
c_2	=	outlet rotor absolute velocity, m/s	Y_{rotor}	=	stagnation rotor pressure drop
ΔS	=	entropy quantity	T^0_w	=	stagnation temperature across rotor
p^0_w	=	stagnation pressure across rotor	h_c	=	stator height, m

1. INTRODUCTION

The design of turbomachinery components is based on requirements from thermodynamic cycle calculations and analysis. The reminder of this work consists in a preliminary design using a few numerical tools and empirical correlations to obtain the main geometrical data of turbomachinery. Reduced-order models have been vastly studied and analyzed by a number of researcher communities on turbomachinery since it plays a very strong whole to obtain an accurate result using empirical models obtained from several test cases, (Tomita,2003), (Barbosa,1987) and (Denton,1993). Once aerothermodynamic design point calculations have determined the characteristics of the turbomachinery components (pressure, velocity and temperature distribution along the machine) one should determine main geometrical parameters such as inlet and outlet areas, length, diameter of rotor and stator rows, number of stages and so on. However, most of the time, this results in higher assembly weight and higher working stresses even achieving high efficiency. At this point it may well be found that difficulties arise. Thus, in order to fulfill requirements of design point operation some design parameters must be previously defined from cycle analysis as input data: pressure ratio, rotational speed, inlet and outlet conditions (mass-flow, stagnation properties, velocities or Mach numbers), loss models settings to account the internal viscous effects, shock waves, endwall, profile losses, secondary losses, Reynolds number correction due to the blade surface roughness, clearance effects and others depending on the specific characteristics of the component. Moreover, the aerodynamic design of the turbomachinery must take into account manufacturing feasibility from the outset. The mechanical design can start only after the thermodynamic and aerodynamic design teams have established the complete calculations and dimensions of the engine. It will then probably be found that stress or vibration problems may lead to further changes of requirements of mechanical stress. Mostly, it is often an interactive process for designers due to the complex inter-rows matching of the turbomachinery design, specially, for multistage machines as axial compressors (Tomita and Barbosa, 2003a , Tomita and Barbosa, 2003b) and steam turbines. Therefore, in Liquid Rocket Engine (LRE) which uses high performance turbo-pumps, some items are strongly important to be considered during the initial arguments on design components due to the high number of physical and mechanical limitations which might change the integrity of a whole system. A basic scheme with after-burned is shown in Fig. 1. (Kessaev, 2009). Usually, all of the fuel and a portion of the oxidizer are fed through the pre-burner to supply power for pumps from turbine. The final selection of the turbine

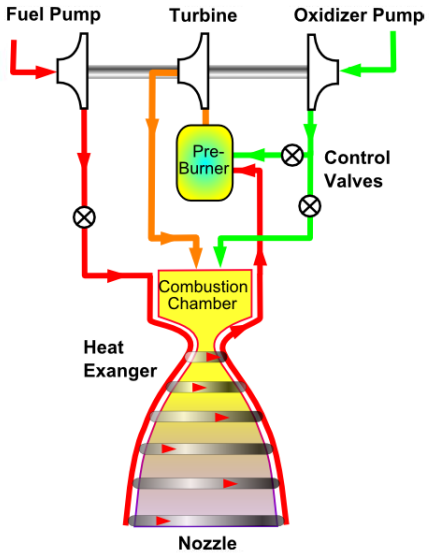

Figure 1. Closed-scheme with after-burned

performance is often a design compromise affected by a number of design requirements. Nowadays, the ad-hoc solution MOEV is becoming useful due to its ability to find a set of optimal solutions, largely known as pareto-optimal solutions, instead of a single optimal solution. It has encouraged the application of MOEV in turbomachinery design. This work apply a fast elitist multi-objective genetic algorithm: NSGA-II, Deb et al. (2000), in a thermodynamic and aerodynamic preliminary design point calculations of a rocket engine with a single-stage axial-flow partial-admission impulse turbine with shroud. (Kopelev and Tikhonov, 1974) , (Ovsyannikov and Borovskii, 1971). The turbo-pump system can be optimized aiming at high efficiency based on particular gas dynamics conditions and low fuel consumption for the same rocket thrust. In addition, the optimization process was driven by the initial conditions of gas dynamics shown in Tab.1. Several methodologies have been applied on rocket design, considering only a single objective function into the genetic algorithm kernel, Srinivas (2005) but only multi-objective methodologies can fufill many design compromises such as those involved in this work.

Table 1. Initial conditions

Variable	Description	Value
G	mass flow rate of working fluid	2.67 [kg/s]
T_0^*	turbine inlet temperature$^\flat$	1000 [K]
P_0^*	turbine inlet pressure$^\flat$	6 [MPa]
P_2	turbine outlet pressure	0.25 [MPa]
R	gas constant	400 [J/kg.K]
k	specific heat ratio$^\flat$	1.33
ω	angular velocity	2410 [rad/s]

($^\flat$): values from a combustion process in gas generator

2. IMPLEMENTATION METHODOLOGY

Evolutionary multi-objective optimization is used to search for multiple Pareto-optimal solutions while numerical optimization algorithms and gradient-based methods have been used to determine the global optimum. Hence, the gradient-based methods are not robust for some engineering problems, (Oyama and Liou, 2001). Thereby finding multiple reliable solutions corresponds to different reliability values. Pareto-optimal sets can be obtained for several sizes, but the size of the Pareto set usually increases with the increase of the objective function numbers, Konak et al. (2006). However, in a constant size (N) of Pareto-optimal solutions, casts doubt on the Pareto-optimal set and tends to give very close solutions regardless of change variability during the selection process of decision variables.

In this study, any serious attempt to find the best parameter settings for real-coded NSGA-II were not done. The number of generations was 2920 with a population size of 1000 candidates. A smaller distribution index $m = 50$ for mutation which has an effect of creating solutions with more spread and an index $c = 20$ for crossover. Furthermore, it has been implemented with a single-point crossover, a SBX operator and polynomial mutation for real-coded genetic algorithms (GAs). Moreover, a crossover probability of ($pc = 0.9$) and a mutation probability ($pm = 1/n$), where n is the number of decision variables for real-coded GAs. A solver for evaluating a set of main objectives in gas dynamic calculation methodology for an impulse turbine type was developed. Its input argument was split into two main parts, decision variables and objective functions, as presented in Fig.2.

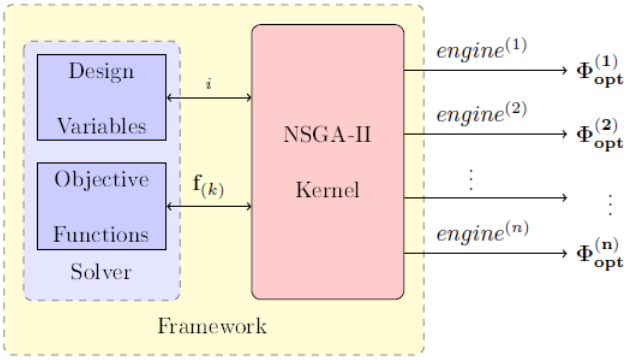

Figure 2. Block diagram of the turbine optimizer

In an NSGA-II, the parent population is used to create an offspring solution similar to a traditional genetic algorithm. Thereafter, both populations are combined and a sorting of the combined population is performed according to an increasing order of domination level. To construct the population for the next generation, solutions from the top of the sorted list are chosen until solutions from the last front cannot be all accepted to maintain the fixed population size. To decide the solutions that should be chosen, a niching strategy is used to choose only those solutions which will make the diversity among them the maximum. The final consideration ensures that a well-diversified set of solutions are found and the emphasis of non-dominated solutions causes a convergence to the Pareto-optimal frontier. The diversity among Pareto solutions was introduced using the crowding comparison procedure, which is used in the tournament selection and during the population reduction phase.

The numerical tool was developed using Matlab 2010a together with the NSGA-II subroutine, based on the work by (Seshadri, 2009). Its flowchart is sketched in Fig.4. Two vectors provide the feeding for the genetic algorithm kernel with

Procedure NSGA-II

Step 1: Create a random parent population P_0 of size N. Set t = 0
Step 2: Apply crossover and mutation to P_0 to create offspring population Q_0 of size N.
Step 3: If the stopping criterion is satisfied, stop and return P_t.
Step 4: Set $R_t = P_t \bigcup Q_t$.
Step 5: Using the fast non-dominated sorting algorithm, identify the non-dominated fronts $F_1, F_2, \cdots, F_k$ in R_t.
Step 6: For $i = 1, \cdots, k$ do following steps :
$\rightsquigarrow$ **Step 6.1:** Calculate crowding distance of the solutions in F_i.
$\rightsquigarrow$ **Step 6.2:** Create P_{t+1} as follows :
1: If $P_{t+1} + F_i \leqslant N$, then set $P_{t+1} = P_{t+1} \bigcup F_i$
2: If $P_{t+1} + F_i > N$, then add the least crowded $N - P_t$ solutions from F_i to P_{t+1}
Step 7: Use binary tournament selection based on the crowding distance to select parents from P_{t+1}. Apply crossover and mutation to P_{t+1} to create offspring population Q_{t+1} of size N.
Step 8: Set $t = t + 1$, and go to Step 3

Figure 3. real-coded NSGA-II: Pseudo code of the algorithm

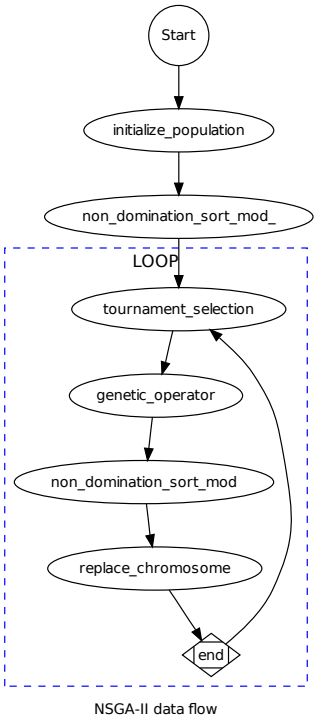

Figure 4. NSGA-II diagram of data flow

the recommended input design parameters (see recommendations in Tab. 2), to the optimization process and the objective functions which drive the flow of the evolutionary algorithm. The latter are conducted by mathematical formulations that proceeds according to minimization or maximization criteria under the design requirements. There is a bidirectional communication between genetic algorithm kernel and solver since for every new generation, new design variables are submitted into and objective functions are again reevaluated . Finally, the last generation get finished a size of (N) best design parameters, or engines, might be evaluated by a local search method based on a weight sum aggregation variant, to deal with the weight reduction requirement. Table 3 describes a list of the main objective functions considered herein. All of them are competing with one another under the context of MOEA. The task is to find as many solutions as possible

such that are optimal or at least acceptable. All simultaneously.

The underlying optimization problem herein is concerned with the pitch-to-chord ratio parameter. There is an optimum value for this relation in which the losses in the cascade are minimum and the number of blades is lower to improve the weight requirements. A high number of blades improve the energy transfer from the gas and avoiding problems with high loading but friction losses between the flow and blade surfaces and the weight of turbine blade row are increased. An optimal value of pitch-to-chord ratio insure a good compromise between energy transfer and weight. Thus, a linear model was purposed to treat with the local search problem within a Pareto-optimal front.

Table 2. Recommendations taken from (Ovsyannikov and Borovskiy, 1971) and (Kopelev and Tikhonov, 1974).

Design variable vector	Bounded parameters	Symbolic variable
x(1)	250 . . . 450	u
x(2)	15 . . . 20	α_1
x(3)	0.001 . . . 0.003	Δ_z
x(4)	10 . . . 15	δ_{seal}
x(5)	0.0016 . . . 0.003	$\delta_r = 20\%$ of x(10)
x(6)	0.001 . . . 0.003	ΔH_p
x(7)	0 . . . 0.001	ΔH_{BT}
x(8)	0.1 . . . 0.15	$\overline{h}$
x(9)	0.033 . . . 0.065	$\overline{b}_{shroud}$
x(10)	0.008 . . . 0.015	b
x(11)	0.02 . . . 0.05	ρ_T
x(12)	-12 . . . 12	ι

2.1 Weight aggregation approach

The representative set of a finite number of solutions requires that the non-dominated solutions are as uniformly as possible distributed on the POF of interest. In order to point out for a reasonable design solution over the space solution, an approach based on the aggregation of weights has been implemented into a model based on sensitive-weight variables, as shows by its functional form Φ^n . The mass of rotating parts were added into a total mass. As such, solutions of POF were sorted increase and hence selected for a desired effective power of 1.2 MW due to pump requirements. Although, it was possible to observe patterns variating in ranges of values for peripheral velocity, effective efficiency and mass.

$$\Phi^n \left(b_p, c_{max}, h_p, z_r, \phi_d, \delta\right)$$

and then, the model gets,

$$\Phi^i = z_r \left[\rho_{b.m} \left\{\left(0.7 b_p c_{max}\right) h_p\right\}\right] + \rho_{d.m} \left\{ \left(\frac{\pi \phi_d}{4}\right)^2 \delta \right\} \tag{1}$$

It was adopted herein for analysis purposes the density of the chrome-nickel steel alloy with $\rho_{.m} = 8880 kg/m^3$ for both blade and wheel of rotor, whereas the reminder parameters,

$$\mathbf{c}_{max} = t - a$$

being, $a = \sigma_2 t q_{(\lambda w2)} \sin \beta_2$, the formula for supersonic discharge velocities and $q_{(\lambda w2)}$ found from gasdynamic function tables as function of outlet relative Mach number M_{w2} for rotor cascades. Let's assume the setting angle equals to 87 degrees.

$$\mathbf{b}_p = \frac{c}{\sin \chi}$$

$$\mathbf{h}_p = \frac{h_{1p} - h_{2p}}{2}$$

$$\mathbf{z}_r = round\left(\frac{\pi D_{cp}}{t}\right)$$

This approach is computationally intensive for bigger population size and exhaustive analysis by a human mind to get in a decision.

3. MATHEMATICAL FORMULATIONS

The main requirement in the design of a turbine for a rocket engine system is the efficient utilization of high-energy working fluid in the smallest obtainable flight-weight configuration. In an axial-flow single-stage impulse turbine, the hot gas supply energy to the blade row that accelerate the flow along with its stream-wise to obtain power on the pumps. The stage efficiency depends upon the energy losses given mostly by empirical or semi-empirical mathematical formulations. It is very difficult to evaluate the effect of each loss source experimentally, since they are physically couple.

Although, the partial-admission is undesirable despite it causes additional energy losses, sometimes its use is unavoidable, since there are applications that, because of limitations imposed by design horsepower, low volumetric gas flow rate and required flow area, would require excessively small blade heights for full-admission (360 degree) nozzle configurations which leads to even greater losses. The losses are divided into the following three basic groups :

i. **Profile losses**

   (a) losses from friction and eddy formation in the boundary layer during its separation.

   (b) edge losses, arising in the vortical trailing wake and during mixing of the flows from pressure and suction surfaces. (horseshoe vortex)

   (c) shock waves and in their interaction with the boundary layer.

   (d) losses due to back-flow.

ii. **End-wall losses**

   (a) from secondary flows (paired vortices), at the stator or rotor cascades and losses in the boundary layer on the end walls.

   (b) from leakage flow at the tip clearance.

   (c) losses from sudden expansion on boundaries of the arc of the intake.

iii. **Additional losses** (*outside the cascade*)

   (a) from friction and eddy formation in the boundary layer on the side walls in the axial clearance (inter-rows).

   (b) from friction of the disk with the gas.

   (c) from leakage flow through the labyrinth seals and slots.

   (d) the effect of disk deflection on axial clearance are of extreme importance to the maintenance of pressure distribution and control of leakage losses.

As the velocity increases, the incidence angle of the flow varies quickly. Hence, it leads to the need for a special profiling of blades for high velocity flow. The nature of the flow path consists of a complex system which requires mostly a depth experimental understanding of many phenomena.

The introduction of the admission degree increases the span of the blade, as Eq. (2). However, a decrease in admission degree leads to an increase in losses connected with admission. Therefore, there is a value of admission degree at which losses in the turbine reach the minimum, and the effective efficiency, the maximum. Nevertheless, the admission degree, once undesirable, will be minimized since its limit will be balanced by an empirical formulation given by the Eq.(8)

$$\epsilon_{opt} = 0.75 \times 10^{-6} \frac{\tau n_{st}^2}{\varphi \left(u/c_{ad}\right)^2 \left(\overline{h}_{opt}\right) \sin \alpha_1} \tag{2}$$

From the above equation and the recommendations given in Tab.2, it will be possible to the evolutionary algorithm approach herein, to achieve a great value without take into account the calculation of the derivative of $\partial \eta_t / \partial \left(h_{1p}/D_{cp}\right) = 0$. The following is the functional form introduced for clarify the important characteristic when considering a global search technique that emulate natural genetic operators. It does not need to assume that the search space is differentiable or continuous.

$$\eta_t = f\left(\frac{h_{1p}}{D_{cp}}, \frac{u}{c_{ad}}, \varphi, \alpha_1, \frac{b}{D_{cp}}, \frac{t}{b}, C_{fdsk}, C_{fsh}, \frac{\Delta}{D_{cp}}\right)$$

This effective efficiency η_T, Eq.(18), will therefore depend on the geometrical correlation of blade length and the corresponding optimal admission degree ε_{opt}, which is involved by the span of the blade of the rotor row. However, both two dependencies are concerned with the peripheral velocity through u/c_{ad}. The evolution approach makes it easier to turn around the complexity of the terms involved in the partial derivative, such as, isentropic velocity ratio $(u/c_{ad})_{opt}$.

The optimum value of the isentropic velocity ratio is decreased with the introduction of partial admission. The height of the rotor blade at the inlet is determined according to value of the height of the stator (h_c) increased by the dimension of the overlaps, Δh_p and Δh_{BT}, see Tab.2 .

$$h_c = \frac{G\sqrt{RT_0^*}}{\epsilon_{opt}\pi D_{cp} p_0 \sigma_1 q_{(\lambda c1)} m \sin\alpha_1} \tag{3}$$

where,

$$m = \sqrt{k\left(\frac{2}{k+1}\right)^{\frac{k+1}{k-1}}}$$

At the low height of rotor cascade, aiming at decreasing vortex pairs losses besides mass reduction, one should minimizing the blade chord, given by Eq.(4) and thus, striving to insure $h_c/b_p > 1$.

$$b_p = \frac{b}{\sin\chi} \tag{4}$$

For short blades it is advantageous to have a closed axial clearance, according to experimental data from (Kopelev and Tikhonov, 1974) it ranges within 20% of the chord. Using shrouds for overlap the vane channel on the periphery and to prevent gas overflow from pressure side to the suction side might increase efficiency but it increases mass and inertial forces. Though, with short blades the secondary losses will be longer the aspect ratio given by Eq.(5) must be maximized in order to decrease such a loss. Conversely, besides the introduction of admission degree to increase the span of the blade of the rotor wheel but with the overlaps introduced into the span of blade, Eq.(6) to insure the unimpeded gas flow from the stator cascade into the rotor wheel, should be somehow close to the aspect ratio in order to reduce the thickness of the wheel b.

$$Aspect\_Ratio = \frac{h_c}{b_p} \tag{5}$$

Herein, let's assume $h_{1p} = h_{2p}$, whereas $h_p = (h_{2p} + h_{1p})/2$.

$$h_{1p} = h_c + \Delta h_p + \Delta h_{BT} \tag{6}$$

It is necessary to keep in mind that with the flow rate through the turbine there is an optimum, with respect to efficiency and admission degree implicit on blade's height. Effective efficiency is increased when volumetric efficiency gets minimum of leakage and in-leakage flow. As such, is desirable to minimize the Eq.(7).

$$\frac{Gy}{G} = \mu_{3a3}\sqrt{1 + \rho_T\left(\frac{1}{\varphi^2\sin^2\alpha_1}\right)}\left(1 + \frac{h_{1p}}{D_{cp}}\right)\frac{\Delta}{h_{1p}} \tag{7}$$

where the coefficient of flow rate of the seal μ_{3a3} can be estimated according to Eq.(8).

$$\mu_{3a3} = \sqrt{\frac{2\delta_r}{1.2\delta_r\delta_{seal}}} \tag{8}$$

Since the flow rate of the seal is determined it is important to maximize the rotor flow rate efficiency defined as it follows.

$$\eta_p = 1 - \frac{Gy}{G} \tag{9}$$

With a decrease in the admission degree, Eq. (2), there will be losses due to friction and admission registered by the lost power given by the Eq.(10), Eq.(11) and Eq.(12). However, as u/c_{ad} increases these power grow according to a cubic dependence.

$$N_{dsk} = 2C_{fdsk}\rho_1 r_2^5\omega^3 \tag{10}$$

$$N_{sh} = C_{fsh}\rho_1 b_s D_2^4\omega^3 \tag{11}$$

The following equation is recommended to estimate the losses from sudden expansion due to partiality acting by an increasing of the rotor vanes.

$$N_{adm} = 0.034\rho_1\frac{h_{1p}}{D_{cp}}\left(1 + 10\frac{b}{D_{cp}}\right)(1 - \epsilon_{opt})\,D_{cp}^5\omega^3 \tag{12}$$

where,

$$Re_{dsk} = \frac{r_2^2 \omega}{\nu}$$

$$Re_{sh} = \frac{D_{sh} \Delta_r \omega}{2\nu}$$

$$C_{fdsk} = \frac{0.039}{Re_{dsk}^{1/5}}$$

$$C_{fsh} = \frac{0.1}{\sqrt{Re_{sh}}}$$

$$r_2 = \frac{D_{cp} - h_{1p}}{2}$$

$$D_{sh} = D_{cp} + h_{1p}$$

The rotor blade inlet angle was obtained from the velocity triangle defined by Eq.(13) while the outlet was obtained from the continuity equation, see Eq.(14)

$$\beta_1 = \arctan\left(\frac{\sin\alpha_1}{\cos\alpha_1 - (u/c_{ad})}\right) \tag{13}$$

In impulse cascades it is advantageous to make the outlet flow angle somewhat within $|\beta_2 - \beta 1| \leq 2$ according to the investigation of a supersonic impulse turbine blade (Hefazi, Kaups and Murry,1995). This will ensure to prevent boundary layer separation and shock reflections through passage through a small convergence of the blade channel which favorably will be reflected on the reduction in the magnitude of those losses. Therefore, is should be minimized.

$$\beta_2 = \arctan\left(\frac{G'\sqrt{RT_{w1}}}{m\epsilon_{opt}\pi D_{cp} p_{w1} \sigma_2 q_{(\lambda w2)} h_{2p}}\right) \tag{14}$$

where the real flow rate is $G' = G - Gy$. The less the outlet flow angle α_1 and β_2, the higher the efficiency since the less the value of the outlet velocity will be and the less the losses with the outlet velocity. In practice, the minimum values of the angles are limited by the fact that with a strong reduction in their values the hydraulic losses increase. Hence, the hydraulic efficiency, Eq.(15), must be maximized to balance such a penalty. At small angles, α_1 and β_2, the profile, secondary and edge losses are increased, since the length of the profile, the flow turning angle and the thickness of the trailing edges in the rotor are increased.

$$\eta_h = \eta_u + \frac{L_c}{L_{ad}^*} \tag{15}$$

In order to ensure high hydraulic efficiency, it is also convenient that the flow turning angle, Eq.(16) be minimized since its magnitude might extend the losses due to friction along the blade passage.

$$\Delta\beta = 180 - (B_{1p} + B_{2p}) \tag{16}$$

where, $B_{1p} = \beta_1 + \iota$ and $B_{2p} = \arcsin\left(\frac{a}{t}\right)$.

The expression below Eq.(17) with the independent selection of degree of reaction ρ_t and outlet flow angle β_2 has an approximate nature, since these two variables should be connected with each other with a change in u/c_1. When $u_2/u_1 = 1$ we obtain the following expression for the circular efficiency of an axial stage of the turbine considering the introduction of the small reaction in the rotor row, since at supersonic velocities at outlet the flow pattern in the partial stage is changed. The range for such a reaction degree is given in Tab.2. Let's consider the derivative of the circular efficiency in another form, where $u_1 = u_2 = u$ and $w_2 = \psi w_1$, whereas $w_1 = c_1 \cos\alpha_1 - u$.

$$\eta_u = 2\varphi^2 \frac{u}{c_1}(1 - \rho_T)\left[\cos\alpha_1 + \psi\cos\beta_2\sqrt{1 + \frac{\rho_T}{\varphi^2(1-\rho_T)} + \left(\frac{u}{c_1}\right)^2 - 2\frac{u}{c_1}\cos\alpha_1} - \left(\frac{u_1}{c_1}\right)\right] \tag{17}$$

In connection with impulse turbines it is advantageous to have the introduction of small reaction degree, or additional work of volumetric expansion, ρ_T within $0.02 \ldots 0.05$. The lost work due to friction with the gas flow along the blades of rotor cascade, especially at constant pressure as usual for impulse cascades, turns into heat, becoming an irreversible loss of mechanical energy. It can be computed by Eq.(24). In practice at supersonic velocities of the outflow during partial admission is changed and then an impulse rotor cascade in calculation will operate as a reaction cascade. Actually, for axial-flow impulse turbines with partial admission and degree of reaction exceeding 0.05 will be accomplished by great losses.

$$\eta_T = \frac{N_T}{GL_{ad}^*} \tag{18}$$

The value of the circular efficiency defines the effective efficiency of the turbine, Eq.(18) and therefore both must be maximized. As a rule, a circular efficiency takes into account full gas feed along the circumference of the wheel ($\epsilon = 1$) and therefore do not have the additional disk losses connected with the admission. Figure 5 shows a comparative analysis with a full gas feed in the wheel circumferential direction.

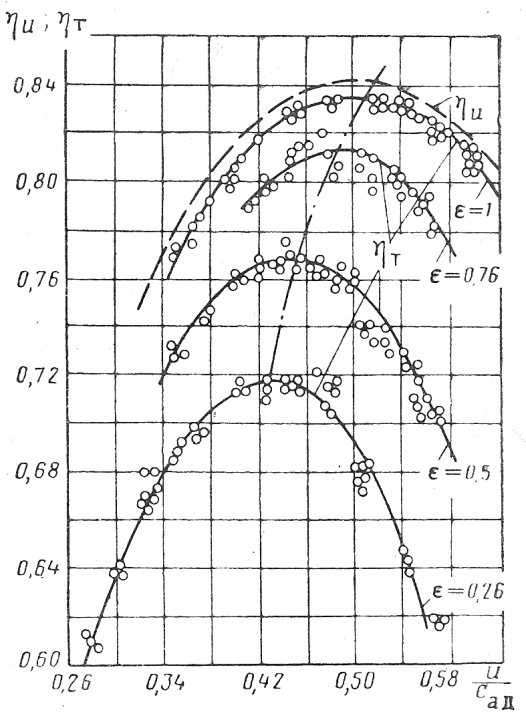

Figure 5. Experimental dependence of the efficiency of a single-stage turbine on isentropic velocity ratio at different values of the admission degree.

The introduction of partial admission due to small volumetric flow rate of gas , considered by autonomous turbines of liquid-propellant rocket engine, leads to a drop in efficiency of the turbine connected to hydraulic losses and losses with discharge velocity considered by the circular efficiency. As shown in Eq.(19), profile losses and secondary losses, will be lowered noticeably with a decrease in the height of the blades. For real turbines a growth in η_u with an increase in ρ_t will be observed since an increasing of the coefficients of velocity φ and ψ with the introduction of degree of reaction due to enough less outlet velocities from stator towards the inlet of rotor cascade. The expression for the velocity coefficient of rotor blades ψ with a shroud at supersonic velocities can approximately be presented in the form :

$$\psi = \left[1 - 0.23\left(1 - \frac{\beta_1 + \beta_2}{\pi}\right)^3\right]\left[1 - 0.05\left(M_{w1} - 1\right)^2\right]\left[1 - 0.06\frac{b}{h_{1p}}\right]\left[1 - \frac{t}{2\pi D_{cp}\epsilon}\right] \tag{19}$$

The first term considers friction losses and vortex formation during the flow around the rotor blade, the second term - the shock wave losses, the third term - tip losses in the rotor cascade, and the fourth term - losses connected with the gas overflow in a circular direction. In addition, edge losses arises as a result of the interaction of boundary layers flowing from the pressure side of turbine blade. Usually, it depends on the boundary layer state at the trailing edge and hence with boundary layer separation and the edge losses increase sharply, (Kopelev and Tikhonov,1974) . With an increase in M_{w1}, losses due to vortex pair are decreased, since the boundary layer thickness on the limiting surfaces and blades are decreased. Thus, the rotor cascade efficiency can be expressed by the following equation :

$$\eta_2 = \psi^2 = 1 - \xi_{rotor} \tag{20}$$

Losses connected with the finite length of the blade, mainly losses to the vortex pair, can be taken into account by a decrease in the efficiency of the rotor cascade. For small values of outlet angles, the profile, secondary and edge losses are increased since the length of the profile, the turning angle and the thickness of the trailing edge in the plane of rotation are increased. According to (Ovsyannikov and Borovskii, 1971), for a decrease in the mass of the construction and reduction in the flow rate of working-fluid, it is necessary to have high coefficient of circular work, Eq.(21). This is especially important for autonomous turbines of liquid-propellant rocket engines, as depicted in Fig. 6. The coefficient of circular

work define by the following equation characterizes the degree of use of the permissible peripheral velocity u. The permissible value of the peripheral velocity u of turbines of LPRE makes influences on the overall dimensions. Hence, operating at high peripheral velocity implies in a higher efficient engine whereas penalizing by a structural standpoint. This is an important design compromise for autonomous turbines. This work assumes the gas conditions for the adiabatic work L^*_{ad} to be constant or fixed previously, according to Tab.1 and deals on a range of permissible peripheral velocities as indicated in the Tab.2.

$$\overline{L}_u = \frac{\eta_u}{2\left(u/c_{ad}\right)^2} \tag{21}$$

Finally, the effective power of the turbine will be given by a design requirement which comes from an energy balance of the overall turbo-pump. The overall dimensions and mass of the turbine should be minimum to supply a gain in power-to-weight ratio and thus, increase the performance of the engine. However, many design parameters and objectives come up with many trades-off decisions which become the procedure a time-consuming task.

Once the circular work L_u of the rotor wheel is less than the available energy of the gas L^*_{ad} due to losses of energy in the stator, losses in the rotor and losses with the outlet velocity L_c is writen as:

$$L_u = L^*_{ad} - L_\varphi - L_\psi - L_c \tag{22}$$

where, L^*_{ad} is the adiabatic work available whereas $\delta_P = p0/p2$ the pressure ratio across turbine. Turning to the losses of energy at the outlet of stator and rotor row, Eq.(23) and Eq.(24) respectively, implies in minimizing the following equations.

$$L_\varphi = \frac{c^2_{1ad}}{2} - \frac{c^2_1}{2} \tag{23}$$

$$L_\psi = \frac{w^2_1}{2} - \frac{w^2_2}{2} \tag{24}$$

Although, the kinetic energy of the fluid, calculated from the outlet velocity of a particular channel, Eq.(25) especially in turbines of liquid-propellant rocket engines, is conditionally taken as the lost energy. This energy can be considered as lost in the sense that it cannot be converted into the useful work. Such a loss, which is called high-speed outlet loss, is calculated according to the escape velocity of the gas from the channel and is also must be minimized.

$$L_c = \frac{c^2_2}{2} \tag{25}$$

and the, adiabatic work given by

$$L^*_{ad} = \frac{k}{k-1} RT_0 \left(1 - \frac{1}{\delta_P^{\frac{k-1}{k}}}\right)$$

Although, as no work is done by the gas relative to the blades, $T^0_{w1} = T^0_{w2}$. The loss coefficient in terms of pressure drop due to losses along the rotor blades is defined by Eq.(26) and also needs to be maximized while the entropy generated might be minimized by the Eq.(27).

$$Y_{rotor} = \frac{p^0_{w1} - p^0_{w2}}{p^0_{w2} - p_2} \tag{26}$$

$$\Delta S = -R \ln \sigma^2 \tag{27}$$

where the total pressure drop of rotor is given by Eq.(28)

$$\sigma_2 = \left(\frac{1 - \left(\frac{k-1}{k+1}\right)\left(\frac{\lambda_{w2}}{\psi}\right)^2}{1 - \left(\frac{k-1}{k+1}\right)\lambda^2_{w2}} \right)^{\frac{k}{k-1}} \tag{28}$$

Therefore, the effective power of the turbine is given by Eq.(29).

$$N_T = (G - Gy)\, L_u - N_{dsk} - N_{sh} - N_{adm} \tag{29}$$

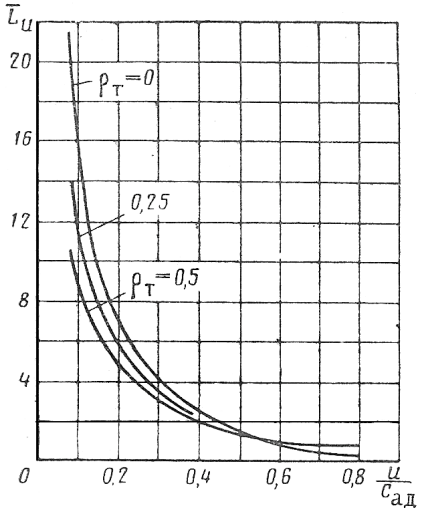

Figure 6. Dependence of $\overline{L}_u$ on u/c_{ad} and ρ_T.

4. RESULTS

Solutions were firstly sorted by mass increase and hence, searched by a power-balance requirement of 1.2 MW with peripheral velocity within strenght conditions between 250 to 300 m/s . The sorted resultant vector shown ranges of patterns for a effective efficiency, peripheral velocity and mass. Thus, is was observed solutions of range:

- between 6 to 15 kg with,
- coefficients of $\overline{L}_u$ between 4.39 to 6.76,
- effective efficiencies between 0.45 to 0.49 .
- solutions out of range in peripheral velocity exhibited lower coefficients of $\overline{L}_u$ and hence, are heavier.
- finally, the highest efficiency and power found, both peripheral velocity and mass always will increase.

Table 3 shows two solutions taken from these observations. A final decision must be taken from a particular need based on the other design objectives. Once the effective efficiency objective depend linearly of all the others, the meaning of its stagnation shows how changes in maximum effective efficiency has been influenced generation by generation up to converge. This proves somehow the effectiveness of the guidance of every objective function to the Pareto-optimal front. Figure 7 demonstrates a convergence stagnated at limited effective efficiency of 0.5286 achieved to this work as one example of the evolution process.

Although, the present analysis it is not enough to fulfill requirements from a structural standpoint since doubts arise due to inertial displacements of centrifugal forces, it suggests new insights into a real world design as well as new models to evaluate them. Unfortunately, centrifugal forces and vibrations are beyond the scope of this paper and they will be reported as a future work.

5. CONCLUSION

A single-stage axial-flow impulse turbine with shroud has been purposed to be optimized by a multi-objective evolutionary algorithm. It was used the well-known real-coded NSGA-II which obtained an uniform Pareto-optimal set that include designs outperforming traditional ones during a preliminary phase, concerning with performance and weight. For aerospace applications requirements of power-to-weight ratio gets higher magnitudes since the priority at handy is achieved by highest coefficient of circular work but under penalties of minimum performance characteristics resumed by a low effective efficiency. Special attention in preliminary design of supersonic rocket turbine engine has been done taking into account different scenarios in design compromise settings. Herein, the simulations shown, in most designs conditions that the flows were found to be highly sensitive to small changes in geometry which purpose future works involving them. The rapidly growing interest in the area of MOEAs is reflected by several works dedicated to this subject with applications on turbomachinery. This work reinforces that it is impractical to analyze higher dimensional interactions without enough constraints. Finally, it is important during preliminary phase to explore the solution space before committed to any subset of the solutions that appears to be promising. The present paper considered a non-multidisciplinary environment.

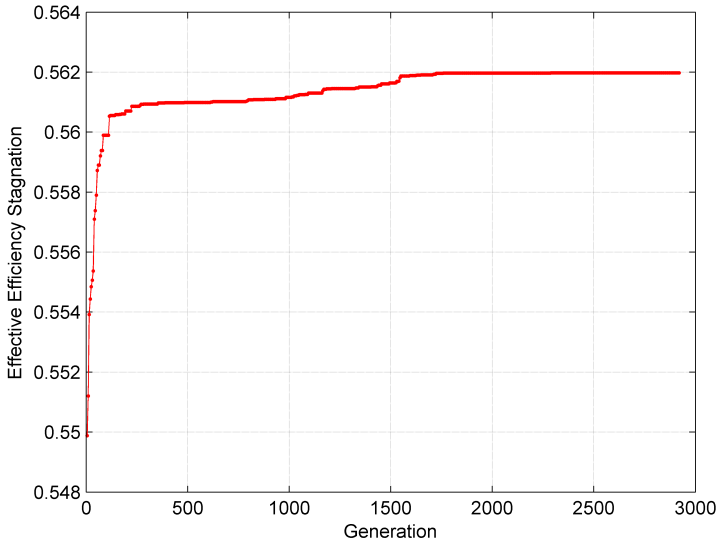

Figure 7. Stagnation of maximum effective efficiency from the Pareto-optimal front obtained.

Table 3. Design Performance

	Description	**Criteria**	**H.E.S.**$^{(a)}$	**L-W.S.**$^{(b)}$
1	Empirical correlation for the attack angle	minimize	0.026757	0.32995
2	Blade chord [m]	minimize	0.008011	0.012779
3	Partial admission degree	minimize	0.23063	0.3598
4	Aspect ratio	maximize	3.9877	1.9896
5	Leakage over shroud [kg/s]	minimize	0.013342	0.054087
6	Rotor flow rate efficiency	maximize	0.98666	0.94591
7	Outlet flow angle [degree]	minimize	0.41807	0.37351
8	Blade deflection angle [degree]	minimize	151	160.95
9	Rotor row efficiency	maximize	0.74081	0.68143
10	Circular efficiency	maximize	0.64189	0.50552
11	Loss kinetics in conical passage [J/kg]	minimize	1.0031×10^5	97366
12	Loss kinetics in rotor passage [J/kg]	minimize	88165	1.0469×10^5
13	Loss kinetics in outlet of rotor blade [J/kg]	minimize	1.0882×10^5	1.8579×10^5
14	Circular work [J/kg]	maximize	5.821×10^5	4.9155×10^5
15	Circular specific work [J/kg]	maximize	4.1755	6.3751
16	Lost power in partial admission [W]	minimize	1.6684×10^5	41064
17	Lost power with disk friction [W]	minimize	2777.6	631.99
18	Lost power with shroud friction [W]	minimize	443.36	235.46
19	Hydraulic efficiency	maximize	0.78567	0.77023
20	Effective power [W]	maximize	1.3634×10^6	1.1995×10^6
21	Effective efficiency	maximize	0.562	0.46032
22	Circular power [W]	maximize	1.5542×10^6	1.3124×10^6
23	Effective work [J/kg]	maximize	5.1064×10^5	4.4926×10^5
24	Pressure drop coefficient across rotor blades	maximize	0.69199	0.74656
25	Entropy across rotor blades	minimize	158.99	182.58

$^{(a)}$ Highest Efficient Solution
$^{(b)}$ Light-Weight Solution

6. ACKNOWLEDGEMENTS

It is a pleasure to acknowledge the help of many people who made this work possible. I am thankful to the support by federal grants CAPES/CNPq and Brazilian Space Agency - AEB from Institute of Aeronautics and Space - IAE/DCTA

to the Liquid Propulsion Laboratory - LPL/IAE as a part of a long-term aerospace research program in Moscow Aviation Institute - MAI, Russia. I would like to express my profound gratitude and appreciation to Professor Serguei Timouchev at MAI by his lectures in turbopump unit. I would like to thank Professor Jesuino Takachi Tomita of the Center of Gas Turbine and Energy of Technological Institute of Aeronautics - ITA for his constant trust, understanding and support.

7. REFERENCES

Barbosa, J. R., 1987, Phd Thesis, “A Streamline Curvature Computer Programme for Performance Prediction of Axial Flow Compressors" , Cranfield Institute of Technology .

Deb, K. and Pratap, A. and Agarwal, S. and Meyarivan, T., 2000, “A Fast Elitist Multi-Objective Genetic Algorithm: NSGA-II" , IEEE Transactions on Evolutionary Computation, Vol. 6, pp. 182-197.

Denton, J., 1993, “Loss Mechanisms in Turbomachines", Jornal of Turbomachinery, Vol. 115, pp. 621-656.

Tomita, J.T., 2003, MSc Thesis, “Numerical Simulation of Axial Flow Compressors" , Technological Institute of Aeronautics - ITA/CTA-Brazil, pp 151.

Tomita, J. and Barbosa, J., 2003, “A Model for Numerical Simulation of Variable Stator Axial Flow Compressors" , Proceedings of COBEM, 17th International Congress of Mechanical Engineering. ABCM, COB01-0239.44

Tomita, J. and Barbosa, J., 2004, “Design and Analysis of an Axial Flow Compressor for a 1MW Gas Turbine", Proceedings of ENCIT, 10th Brazilian Congress of Thermal Sciences and Engineering - ENCIT, CIT04-0062.44.

Hefazi, H., Kaups, K. and Murry, R.,“ A Computational Study of Flow Over a Supersonic Impulse Turbine Blade", 26th AIAA Fluid Dynamic Conference, AIAA 95-2287,San Diego, June 1995.

Jin, Y., “Effectiveness of weighted sum of the objectives for evolutionary multi-objective optimization: Methods, analysis and applications", Unpublished manuscript, 2002.

Jin, Y. and Sendhoff , B., “Connectedness, regularity and the success of Local Search in Evolutionary Multi-Objective Optimization", in Proceedings of the Congress on Evolutionary Computation, IEEE Press, pp. 1910-1917, 2003.

Kessaev, K. V. , 2009, “Theory of Liquid-propellant Rocket Engine", Moscow Aviation Institute - MAI , Moscow.

Konak, A. and Goit, D. W. and Smith, A. E., 2006, “Multi-objective Optimization using Genetic Algorithms: A tutorial", Reliability Engineering & System Safety, Vol. 91, n. 17, pp. 992-1007.

Kopelev, S. Z. and Tikhonov, N. D., 1974 ,“Raschet turbin aviatsionnykh dvigateley (gazodinamicheskiy raschet. profilirovaniye lopatok)", Mashinostroyeniy, Moscow, pp. 268.

Obsyannikov, B. V. and Borovskiy, B. I., 1971, “Teoriya i Raschet Agregtov Pitaniya Zhidkostnykh Raketnykh Dvigatelei", Mashinostroyeniy, Moscow, pp. 539.

Oyama, A. and Liou, M., 2001, “Multiobjective Optimization of Rocket Engine Pumps Using Evolutionary Algorithm",NASA Glenn Research Center, NASA/TM-2001-211082, also AIAA Paper 2001-2581.

Srinivas, 2005, “Optimum Design of Axial-flow Gas Turbine Stage using Genetic Algorithms", Institution of Engineers INDIA,Vol. 85, pp.179-187.

8. Responsibility notice

The author(s) is (are) the only responsible for the printed material included in this paper